

EARLY RADIO AND X-RAY OBSERVATIONS OF THE YOUNGEST NEARBY TYPE Ia SUPERNOVA PTF 11kly (SN 2011fe)

ASSAF HORESH¹, S. R. KULKARNI¹, DEREK B. FOX², JOHN CARPENTER¹, MANSI M. KASLIWAL^{1,3}, ERAN O. OFEK^{1,4},
ROBERT QUIMBY⁵, AVISHAY GAL-YAM⁴, S. BRADLEY CENKO⁶, A. G. DE BRUYN^{7,8}, ATISH KAMBLE⁹, RALPH A. M. J. WIJERS⁹,
ALEXANDER J. VAN DER HORST¹⁰, CHRYSsa KOUVELIOTOU¹¹, PHILIPP PODSIADLOWSKI¹², MARK SULLIVAN¹²,
KATE MAGUIRE¹², D. ANDREW HOWELL^{13,14}, PETER E. NUGENT¹⁵, NEIL GEHRELS¹⁶, NICHOLAS M. LAW¹⁷,
DOVI POZNANSKI¹⁸, AND MICHAEL SHARA¹⁹

¹ Cahill Center for Astrophysics, California Institute of Technology, Pasadena, CA 91125, USA

² Astronomy and Astrophysics, Eberly College of Science, The Pennsylvania State University, University Park, PA 16802, USA

³ Carnegie Institution for Science, 813 Santa Barbara Street, Pasadena, CA 91101, USA

⁴ Benoziyo Center for Astrophysics, Faculty of Physics, The Weizmann Institute of Science, Rehovot 76100, Israel

⁵ IPMU, University of Tokyo, Kashiwanoha 5-1-5, Kashiwa-shi, Chiba, Japan

⁶ Department of Astronomy, University of California, Berkeley, CA 94720-3411, USA

⁷ Netherlands Institute for Radio Astronomy (ASTRON), Postbus 2, NL-7990 AA Dwingeloo, The Netherlands

⁸ Kapteyn Astronomical Institute, University of Groningen, Postbus 800, NL-9700 AA Groningen, The Netherlands

⁹ Center for Gravitation and Cosmology, University of Wisconsin, Milwaukee, WI 53211, USA

¹⁰ Universities Space Research Association, NSSTC, Huntsville, AL 35805, USA

¹¹ Space Science Office, VP-62, NASA-Marshall Space Flight Center, Huntsville, AL 35805, USA

¹² Department of Physics (Astrophysics), University of Oxford, Keble Road, Oxford OX1 3RH, UK

¹³ Las Cumbres Observatory Global Telescope Network, Santa Barbara, CA 93117, USA

¹⁴ Department of Physics, University of California Santa Barbara, Santa Barbara, CA 93106, USA

¹⁵ Computational Cosmology Center, Lawrence Berkeley National Laboratory, 1 Cyclotron Road, Berkeley, CA 94720, USA

¹⁶ NASA-Goddard Space Flight Center, Greenbelt, MD 20771, USA

¹⁷ Dunlap Institute for Astronomy and Astrophysics, University of Toronto, 50 St. George Street, Toronto, Ontario M5S 3H4, Canada

¹⁸ School of Physics and Astronomy, Tel-Aviv University, Tel-Aviv 69978, Israel

¹⁹ Department of Astrophysics, American Museum of Natural History Central Park West & 79th Street, New York, NY 10024, USA

Received 2011 September 13; accepted 2011 October 25; published 2012 January 20

ABSTRACT

On 2011 August 24 (UT) the Palomar Transient Factory (PTF) discovered PTF11kly (SN 2011fe), the youngest and most nearby Type Ia supernova (SN Ia) in decades. We followed this event up in the radio (centimeter and millimeter bands) and X-ray bands, starting about a day after the estimated explosion time. We present our analysis of the radio and X-ray observations, yielding the tightest constraints yet placed on the pre-explosion mass-loss rate from the progenitor system of this supernova. We find a robust limit of $\dot{M} \lesssim 10^{-8} (v/100 \text{ km s}^{-1}) M_{\odot} \text{ yr}^{-1}$ from sensitive X-ray non-detections, as well as a similar limit from radio data, which depends, however, on assumptions about microphysical parameters. We discuss our results in the context of single-degenerate models for SNe Ia and find that our observations modestly disfavor symbiotic progenitor models involving a red giant donor, but cannot constrain systems accreting from main-sequence or sub-giant stars, including the popular supersoft channel. In view of the proximity of PTF11kly and the sensitivity of our prompt observations, we would have to wait for a long time (a decade or longer) in order to more meaningfully probe the circumstellar matter of SNe Ia.

Key words: radio continuum: general – supernovae: general – X-rays: general

Online-only material: color figures

1. INTRODUCTION

Type Ia supernovae (SNe Ia) have served as an exquisite probe of cosmography (Riess et al. 1998; Perlmutter et al. 1999). As a result of this role, this class has been studied in unprecedented depth and breadth. Nonetheless the progenitors of SNe Ia remain enigmatic. According to common wisdom, an SN Ia is due to the thermonuclear explosion of a white dwarf with a mass approaching the Chandrasekhar limit (Hoyle & Fowler 1960). The progenitor question is then one of understanding how a white dwarf can approach the Chandrasekhar mass (see review by Hillebrandt & Niemeyer 2000). In the single-degenerate (SD) model (Whelan & Iben 1973), a white dwarf (WD) accretes mass from its hydrogen-rich star companion, reaches a mass close to the Chandrasekhar mass, which is sufficient to ignite carbon, and explodes. In the double-degenerate (DD) model, a supernova (SN) results from the merger of two WDs (Iben & Tutukov 1984; Webbink 1984; see also Yungelson & Livio 2000).

It has long been suggested that radio and X-ray observations of SNe Ia have the ability to provide diagnostics to distinguish between these two models (Boffi & Branch 1995; Eck et al. 1995; Panagia et al. 2006). In most variations of the SD model, the winds from the donor star will enrich the circumstellar medium (CSM). The interaction of the blast wave from the SN with the CSM can result in radio emission. In contrast, there is no expectation of CSM and hence of radio emission in the DD model.

On UTC 2011 August 24.16 the Palomar Transient Factory (PTF; Law et al. 2009; Rau et al. 2009) discovered PTF 11kly, a rapidly rising transient, in the nearby (distance $d \approx 6.4$ Mpc; Shappee & Stanek 2011) galaxy Messier 101 (Nugent et al. 2011). Spectroscopy undertaken at the Liverpool Telescope led to a plausible Ia classification²⁰ and was soon confirmed

²⁰ At which point the event was rechristened to SN 2011fe by the Central Bureau for Astronomical Telegrams.

Table 1
Log of Radio Observations

Start (UT)	ΔT (day)	τ (minute)	Facility	ν (GHz)	S_ν (μJy)	Luminosity ($\lesssim 10^{24} \text{ erg s}^{-1} \text{ Hz}^{-1}$)	\dot{M} ($10^{-8} w_7 / \epsilon_{-1} M_\odot \text{ yr}^{-1}$)	Note
Aug 24.98	1.4	178	CARMA	93	-16 ± 510	75	23	(1)
Aug 25.02	1.3	37	EVLA	8.5	-4.4 ± 25	3.7	1.7	(2)
Aug 27.71	4.0	35	EVLA	5.9	1.3 ± 7	1.0	1.1	(3)
Aug 28.25	4.8	800	WSRT	4.9	-71 ± 34	5.0	2.6	(4)
Aug 29.97	6.3	29	EVLA	5.9	-0.9 ± 9	1.3	3.1	(3)
Aug 31.38	8	630	WSRT	1.4	2 ± 25	3.7	1.7	(4)

Notes. The columns starting from left to right are as follows: start of integration in UT; mean epoch of observation (in days since explosion); integration time in minutes; facility; central frequency in GHz; nominal flux and associated rms in the vicinity of PTF11kly in μJy ; the corresponding 3σ spectral luminosity assuming a distance of 6.4 Mpc to M101; inferred upper limit to the mass-loss rate (see Section 3.1 for explanation of parameters); specific notes (see below). Following Nugent et al. (2011) we assume that the explosion time of PTF11kly is UT 2011 August 23.69. The following packages were employed to reduce the data: AIPS (EVLA), Miriad (CARMA), and NEWSTAR (WSRT). (1) The CARMA observations were obtained in the E configuration using only nine 6 m antennas. The larger antennas were not available owing to reconfiguration of the array. Bandwidth of 8000 MHz. Calibrators: J1153+495 and J1642+689 (phase) and MWC349 (flux). (2) Bandwidth of 256 MHz. Calibrators: J1419+5423 (phase) and 3C286 (flux). (3) Bandwidth of 2000 MHz. Data obtained under Director’s discretionary time (PI: A. Soderberg). (4) Bandwidth of 8×20 MHz. For each of the eight IF channels, only 3/4 of the channel bandwidth was used in making the map. The flux density calibrators used were 3C147 and 3C286 on the Baars et al. (1977) scale.

by observations at the Lick 3 m telescope and the Telescopio Nazionale Galileo.

The apparent extraordinary youth and the proximity²¹ of PTF 11kly presents a unique opportunity to sensitively probe the CSM of an SN Ia. Therefore, we immediately initiated (Gal-Yam et al. 2011) observations with the *Swift* Observatory, the Combined Array for Research in Millimeter-wave Astronomy (CARMA)²² and the Expanded Very Large Array (EVLA).²³ A few days later low-frequency observations were undertaken at Westerbork Synthesis Radio Telescope (WSRT).²⁴ X-ray observations were obtained with the *Swift* and *Chandra* observatories.

2. THE OBSERVATIONS

The early optical light curve of PTF11kly shows an extraordinary good fit to that expected from an exploding star (flux proportional to exponential of square of time). As a result the birth of the SN can be accurately timed to a fraction an hour: UT 2011 August 23.69 (Nugent et al. 2011). Our first observations at both radio and X-ray bands were taken just over a day after the explosion.

2.1. Radio

The log of observations and the associated details can be found in Table 1. Our CARMA and EVLA observations include the earliest search for radio emission in centimeter-wave and millimeter-wave bands and subsequent observations include a very sensitive search in the 21 cm band obtained at the WSRT (see Figure 1). Following our first EVLA and CARMA

observations, an additional datum was taken at a lower frequency (5 GHz) on UT 2011 August 25.8 by Chomiuk & Soderberg (2011). They reported a null detection with $-5 \pm 6 \mu\text{Jy}$. As can be gathered from Table 1 there are no detections at any epoch and in any band. In the next section we discuss the implications of these null detections.

2.2. X-Ray Observation

Following our classification of PTF11kly as an SN, we immediately triggered the *Swift* Observatory (see log of observations in Table 2). The first *Swift* observations²⁵ began on UT 2011 August 24.92. We used the *Swift* X-Ray Telescope (XRT) data products generator of the UK *Swift* Science Data Centre (SSDC; see Evans et al. 2009) to generate a single combined and astrometrically corrected event file from the first 58.2 ks of exposure. Six events are found within an aperture of radius 9 XRT pixels ($21''/2$) centered on the position of PTF11kly. This can be compared to independent background expectations of 7.0 ± 0.4 and 11.7 ± 0.7 counts, respectively. The corresponding 90% confidence limits on total source counts and aperture-corrected average count rate are $n_\gamma < 4.3$ and $r_X < 0.1 \times 10^{-3} \text{ s}^{-1}$, respectively.

However, we note that two of the counts within the source region arrive within the first 2 ks—an a priori unlikely occurrence (at $\approx 90\%$ level of confidence)—and could be taken as evidence of early, bright X-ray emission from PTF 11kly, at the $L_X \sim 10^{38} \text{ erg s}^{-1}$ level (see also Fox 2011a, 2011b). We realize that this statistical evidence does not warrant a claim of detection. Nonetheless, given that the observations were done at an extraordinarily early epoch of 1.21 days post-explosion, we think it worth highlighting this issue for the benefit of future observers.

Our upper limit of $n_\gamma < 4.8$ counts, from the first *Swift* observation sequence (4.5 ks exposure) alone, provides the following upper limits on X-ray flux (over the energy range 0.3–10 keV)²⁶: $F_X < 6.2 \times 10^{-14} \text{ erg cm}^{-2} \text{ s}^{-1}$ (thermal bremsstrahlung model with $kT = 10 \text{ keV}$) and $F_X < 5.0 \times$

²¹ The closest SN Ia previous to PTF 11kly is 1986G at a distance of 5.5 Mpc.

²² Support for CARMA construction was derived from the states of California, Illinois, and Maryland, the James S. McDonnell Foundation, the Gordon and Betty Moore Foundation, the Kenneth T. and Eileen L. Norris Foundation, the University of Chicago, the Associates of the California Institute of Technology, and the National Science Foundation. Ongoing CARMA development and operations are supported by the National Science Foundation under a cooperative agreement, and by the CARMA partner universities.

²³ The EVLA is operated by the National Radio Astronomy Observatory, a facility of the National Science Foundation operated under cooperative agreement by Associated Universities, Inc.

²⁴ The Westerbork Synthesis Radio Telescope is operated by ASTRON (Netherlands Foundation for Radio Astronomy) with support from the Netherlands Organization for Scientific Research (NWO).

²⁵ Target ID 32081, with initial ObsID 32081001 lasting 4.5 ks over three consecutive orbits, followed by 53.7 ks of observations through September 8.58 (ObsIDs 32081002–32081029).

²⁶ We assume a Galactic interstellar medium contribution of $N_H = 1.8 \times 10^{20} \text{ cm}^{-2}$ (Kalberla et al. 2005). There may be an additional similar contribution from M101, depending on the depth of the line of sight to the SN (Kamphuis et al. 1991).

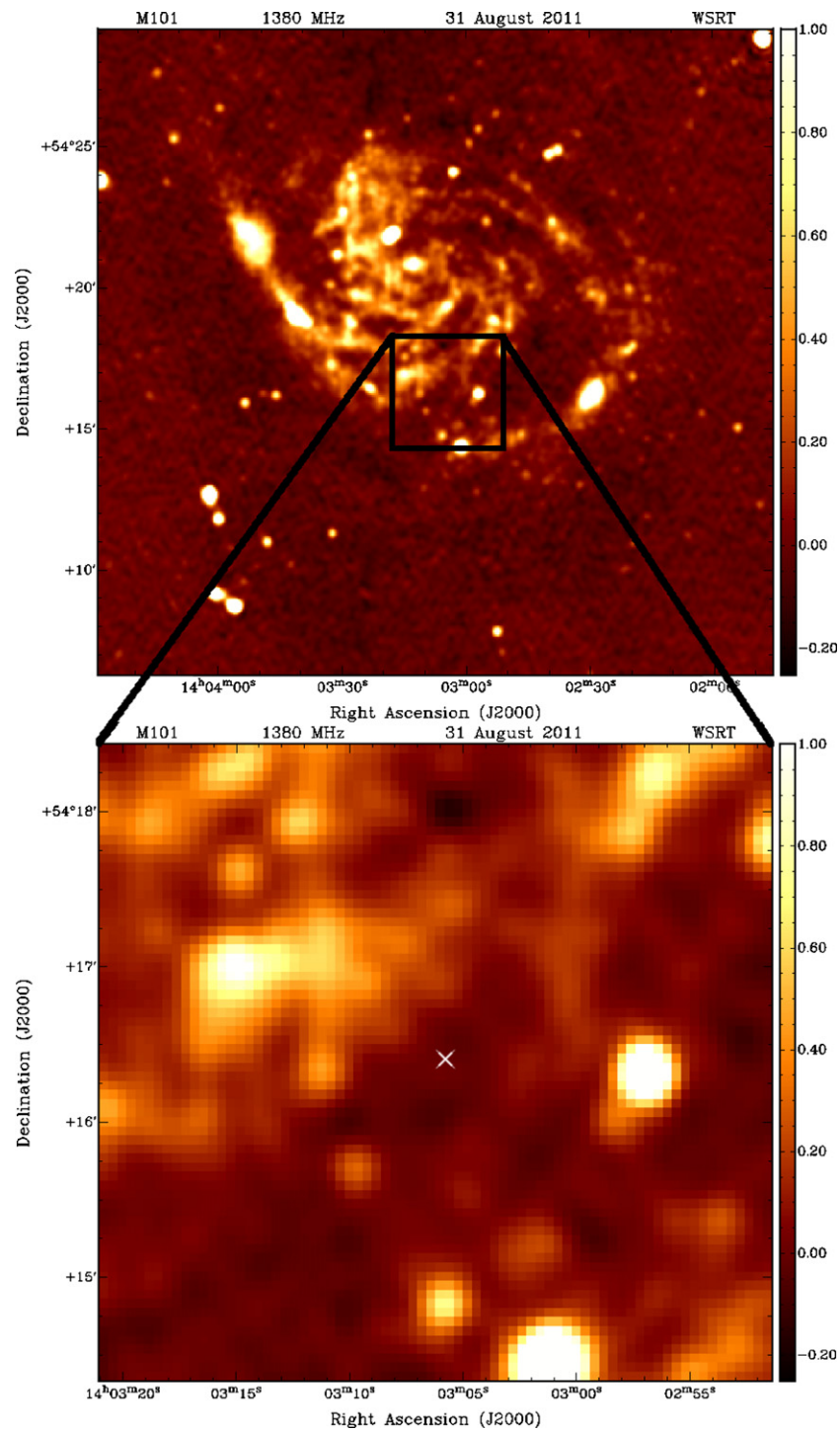


Figure 1. 21 cm image of M101 taken with WSRT on UT 2011 August 31. SN position is shown by the cross. (A color version of this figure is available in the online journal.)

Table 2
Log of X-Ray Observations

Start (UT)	ΔT (day)	τ (ks)	Facility	Band (keV)	F_X ($\lesssim 10^{-16}$ erg cm $^{-2}$ s $^{-1}$)	Luminosity ($\lesssim 10^{36}$ erg s $^{-1}$)	\dot{M} ($10^{-8} w_7 / \epsilon_{e-1} M_\odot$ yr $^{-1}$)
Aug 24.92	1.21	4.5	<i>Swift</i>	[0.3–10]	500	250	20
Aug 27.44	4	49.7	<i>Chandra</i>	[0.3–8]	8.2	4	1.1

Notes. The columns starting from left to right are as follows: start of integration in UT; mean epoch of observation (in days since explosion); integration time in minutes; facility; energy band in keV; flux in 10^{-16} erg cm $^{-2}$ s $^{-1}$; the corresponding luminosity limit assuming a power-law model with photon index $\Gamma = 2$ and a distance of 6.4 Mpc to M101; inferred upper limit to the mass-loss rate (see Section 3.2 for explanation of parameters).

10^{-14} erg cm $^{-2}$ s $^{-1}$ (power-law model with photon index $\Gamma = 2$). Corresponding upper limits to the X-ray luminosity are $L_X < 3.0 \times 10^{38}$ erg s $^{-1}$ and $L_X < 2.5 \times 10^{38}$ erg s $^{-1}$, respectively.

Observations²⁷ with the *Chandra X-Ray Observatory* began on UT 2011 August 27.44 and lasted for 49.7 ks; the mean epoch is UT 2011 August 27.74 (corresponding to 4 days post-explosion; Hughes et al. 2011). No soft proton flaring was evident during the observation. Only one event was found in the source region, a 2.5 arcsec aperture centered on the SN, whereas 2.23 ± 0.1 background counts were expected (in an equivalent aperture). The 90% confidence upper limit on the expectancy value of a Poisson process that generates one count is 3.9 counts. Ignoring the background contribution, after applying the aperture correction (as prescribed by Feigelson et al. 2002), we find an upper limit to the count rate, $r_X \lesssim 0.11 \times 10^{-3}$ s $^{-1}$ (90% confidence).

For the thermal bremsstrahlung model this upper limit translates to $F_X < 9.0 \times 10^{-16}$ erg cm $^{-2}$ s $^{-1}$ (0.3–8.0 keV), corresponding to $L_X < 4.4 \times 10^{36}$ erg s $^{-1}$. For the power-law model we find $F_X < 8.2 \times 10^{-16}$ erg cm $^{-2}$ s $^{-1}$ (0.3–8.0 keV), corresponding to $L_X < 4.0 \times 10^{36}$ erg s $^{-1}$.

3. MASS-LOSS RATE CONSTRAINTS

The theory of radio emission from SNe relevant to Type I events is discussed in Chevalier (1982, 1998) and Chevalier & Fransson (2006), and a summary of radio observations of SNe can be found in Weiler et al. (2002). Panagia et al. (2006) report a comprehensive summary of searches for radio emission from SNe Ia.

The basic physics is as follows. The SN shock wave ploughs through the CSM. In the post-shock layer, electrons are accelerated to relativistic speeds and strong magnetic fields also appear to be generated. The relativistic electrons then radiate in the radio via synchrotron emission. X-rays are emitted via two energy channels: thermal bremsstrahlung emission from hot post-shocked gas and inverse Compton (IC) scattering of the optical photons from the SN by the relativistic electrons.

The density of the CSM is a key physical parameter. After all, a strong shock can only be generated if the SN blast wave can run into the CSM. Thus, the strength of the radio and X-ray emission allows us to diagnose the CSM density.

For a star which has been losing matter at a constant rate, \dot{M} , the circumstellar density has the following radial profile: $\rho(r) = n(r)\mu = \dot{M}/(4\pi r^2 w)$ where w is the wind velocity, r is the radial distance from the star, n is the particle density, and μ is the mean atomic weight of the circumstellar matter. We assume that the circumstellar matter is ionized (by the shock breakout and by radiation from the young SN).

3.1. Constraints from Radio Measurements

Massive stars exploding as SNe Ib/Ic with their fast-moving ejecta and low-density CSM provide a good starting point to discuss radio emission from SNe Ia. The spectrum of the radio emission from SN Ib/Ic events follows the ‘‘Synchrotron Self-Absorption’’ (SSA) form: a $\nu^{5/2}$ low-frequency tail (optically thick regime) and a declining power law, ν^α , at high frequency (optically thin regime). For most well-studied SNe $\alpha \approx -1$. Diagnosis of the CSM is based on the peak frequency (ν_m ; the

synchrotron optical depth is unity at this frequency) and the peak flux (S_m) and the evolution thereof.

We use the basic SSA formulation as in Chevalier (1998) with some modifications (noted below). We assume a fraction of electrons are accelerated to relativistic energies and with a power-law distribution, $dN/dE = N_0 E^{-p}$; here, $E = \gamma m_e c^2$ is the energy of electrons and γ is the Lorentz factor. Electrons which are not relativistic will not radiate strongly and thus we introduce a minimum Lorentz factor, γ_{\min} . Only electrons with $\gamma > \gamma_{\min}$ are assumed to contribute to the radio emission.

As in all strong shocks, in addition to acceleration of electrons, strong magnetic fields appear to be generated in the post-shock gas. Our current understanding is such that we simply parameterize the relative energy fractions of each of these two components.

The thermal energy density of the post-shocked gas is $\frac{9}{8}\rho v_s^2$ (where v_s is the shock speed). The magnetic energy density is $B^2/(8\pi)$. We denote the ratio of this energy density to that of the thermal energy density of post-shocked gas by ϵ_B . We find

$$u_B = \frac{B^2}{8\pi} \approx 6.8 \times 10^9 m^2 \epsilon_B \left(\frac{\dot{M}[M_\odot \text{ yr}^{-1}]}{w[\text{km s}^{-1}]} \right) t_d^{-2} \text{ erg cm}^{-3}; \quad (1)$$

here, m is the power-law exponent in the equation relating the radius of the shock to time, $R_s \propto t^m$, and t_d is the time post-explosion in days. In a similar manner, we let ϵ_e denote the ratio of the energy density of relativistic electrons ($\gamma > \gamma_{\min}$) to the thermal energy density.

The use of radio diagnostics (unfortunately) involves the values of several additional parameters. The first parameter is p , the power-law index of the relativistic electrons. Theory and observations of this value agree that this value should be $p \approx 3$ (see Weiler et al. 2002; Chevalier & Fransson 2006). Next, we make the simplifying assumption that the blast wave moves at a constant velocity, v_s ; this is equivalent to setting $m = 1$. This is admittedly a simplification.²⁸ However, given our non-detections we felt that an analysis more sophisticated than this was not warranted.

Finally, we come to the microphysics parameters, ϵ_e and ϵ_B . It appears from well-studied SN shocks that ϵ_e is usually about 0.1 with modest dispersion (Chevalier & Fransson 2006). In contrast, ϵ_B appears to be a highly variable parameter. This is quite understandable from simple considerations. The magnetic field is generated both in the post-shock gas as well as by compression of the field already present in the pre-shock gas. For instance a radio and X-ray modeling of SN 2002ap (an SN Ic with a presumed Wolf–Rayet progenitor) by Björnsson & Fransson (2004) finds that the assumption of equipartition ($\epsilon_B = \epsilon_e$) leads to inferring \dot{M} much lower than that expected for a Wolf–Rayet progenitor. The inferred mass-loss rate can be increased if $\epsilon_B = 2 \times 10^{-3}$. We find a similar imbalance between ϵ_B and ϵ_e for SN 2011dh (an SN Iib; A. Horesh et al., in preparation; see also Soderberg et al. 2011). For this reason, unless stated otherwise, we will fix $\epsilon_e = 0.1$ and assume that ϵ_B is a free parameter. Finally, since only relativistic electrons contribute to radio and X-ray emission we adopt $\gamma_{\min} = 2$.

²⁸ We are interested in the very outer layers of the exploded star. Note that with (say) a mass-loss rate of $10^{-8} M_\odot \text{ yr}^{-1}$ and a wind velocity of 10^7 cm s $^{-1}$ the leading edge of the shock ($v_s = 4 \times 10^9$ cm s $^{-1}$, say) would have swept up a mere $10^{-8} M_\odot$ by day 1. It is the velocity–density structure of such thin outermost layers that determines v_s .

²⁷ ObsID 14341 (PI: J. Hughes).

Following Chevalier (1998), the radio spectral luminosity in the optically thin regime is given by

$$L_\nu = \frac{(4\pi)^2 f R_s^3}{3} c_5 N_0 B^{(p+1)/2} \left(\frac{\nu}{2c_1}\right)^{-(p-1)/2} \text{erg s}^{-1} \text{Hz}^{-1} \quad (2)$$

and the synchrotron-self-absorbed luminosity is

$$L_\nu = 4\pi^2 f R_s^2 \frac{c_5}{c_6} B^{-1/2} \left(\frac{\nu}{2c_1}\right)^{5/2} \text{erg s}^{-1} \text{Hz}^{-1}, \quad (3)$$

where $R_s = v_s t$ is the shock-wave radius, B is the strength of the magnetic field, and the constants c_1 , c_5 , and c_6 can be found in Pacholczyk (1970). N_0 can be straightforwardly shown to be $\epsilon_e/(8\pi\epsilon_B)B^2(p-2)(\gamma_{\min}m_e c^2)^{p-2}$. Equation (2) can be simplified to yield

$$L_\nu = 3 \times 10^{34} \frac{128\pi^3 f v_s^3}{3} c_5 \gamma_{\min} m_e c^2 \epsilon_e \epsilon_B \left(\frac{\dot{M}[M_\odot \text{yr}^{-1}]}{w[\text{km s}^{-1}]}\right)^2 \times \left(\frac{\nu}{2c_1}\right)^{-1} t_d^{-1} \text{erg s}^{-1} \text{Hz}^{-1}. \quad (4)$$

Given that the earliest observation(s) were undertaken only a day after the explosion, it is prudent to check if there is significant free-free absorption. The free-free optical depth is

$$\tau_{\text{ff}} = 3.3 \times 10^{-7} T_4^{-1.35} \nu_{\text{GHz}}^{-2.1} \text{EM}, \quad (5)$$

where $T = 10^4 T_4$ is the electron temperature (in Kelvin),²⁹ ν_{GHz} is the frequency in GHz, and EM is the emission measure, the integral of n_e^2 along the line of sight in units of $\text{cm}^{-6} \text{pc}$. The emission measure from a radius, say, r_* to infinity is

$$\text{EM} = \int_{r_*}^{\infty} n_*^2 \left(\frac{r}{r_*}\right)^{-4} dr = \frac{1}{3} n_*^2 r_*, \quad (6)$$

where n_* is the density of electrons at radius r_* . Putting these equations together the free-free optical depth is

$$\tau_{\text{ff}} \approx 0.5 \dot{M}_{-8}^2 t_d^{-3} v_9^{-3} w_7^{-2} T_4^{-1.35} \nu_{\text{GHz}}^{-2.1}. \quad (7)$$

For PTF11kly, the photospheric velocity is $v = 2 \times 10^9 \text{ cm s}^{-1}$. The blast wave will at least have this velocity and likely twice this value (Chevalier & Fransson 2006; Fryer et al. 2007; Soderberg et al. 2010). For representative values ($\dot{M} = 3 \times 10^{-7} M_\odot \text{yr}^{-1}$, $w_7 = 1$, $v_9 = 4$) we find the following optical depth at the first epoch of our observations: $\tau_{\text{ff}}[\nu_{\text{GHz}} = 1.4, 5, 8, 95] = [3.5, 0.24, 0.09, 0]$. For interesting values of \dot{M} ($\lesssim 10^{-8} M_\odot \text{yr}^{-1}$) the free-free optical depth is not important for the observations reported here.

Equation (4) provides the starting point for the discussion. This equation shows that the spectral luminosity can constrain \dot{M}/w provided that we have a good grasp of the blast wave dynamics and microphysics of particle acceleration and magnetic field generation. We have argued above that $p \approx 3$, $\epsilon_e \approx 0.1$, and $v_s \approx 4 \times 10^9 \text{ cm s}^{-1}$. We adopt these values and proceed with the discussion.

To start with we can see that the observations reported here (Table 1) yield the lowest limits on the radio luminosity

of very young SNe Ia, $L_\nu \lesssim 10^{24} \text{ erg s}^{-1} \text{Hz}^{-1}$. This limit then constrains the following parameter, $\mathcal{B} \equiv \epsilon \dot{M}/w$, where $\epsilon \equiv \sqrt{\epsilon_B \epsilon_e}$. We have deliberately not quoted the limits on \dot{M} from previous literature since radio measurements yield not \dot{M} but \mathcal{B} and this quantity depends on the unknown parameter, ϵ_B , which (as summarized above) can vary by orders of magnitude. Despite this it is clear that the observations reported here present the most sensitive limits to \dot{M} to date (Figure 2).

From Figure 2 we note that \mathcal{B} can be constrained as follows: the optically thin regime offers a lower bound whereas the optically thick regime (SSA and free-free) an upper bound. The upper bound is not interesting since the simplest explanation for the absence of radio emission is that the explosion takes place in a vacuum (or very low density CSM). Besides, from past studies, there is no indication of \dot{M} in the range of $10^{-6} M_\odot \text{yr}^{-1}$ that is indicated from the upper bounds.

The constraints deduced for each observation are summarized in Table 1. Combining all the constraints we find $\dot{M} \lesssim 1 \times 10^{-8} w_7 (0.1/\epsilon) M_\odot \text{yr}^{-1}$.

3.2. Constraints from X-Ray Data

Past X-ray observations, typically undertaken no earlier than a week past the explosion, have resulted in upper limits at the level of $L_X \lesssim 10^{39} \text{ erg s}^{-1}$. A claim of detection of emission from SN 2005ke ($L_X \sim 2 \times 10^{38} \text{ erg s}^{-1}$; Immler et al. 2006) has been disputed by Hughes et al. (2007). Immler & Russell (2011) reported a detection in a two-month stack of *Swift* XRT data of SN 2011by. However, subsequent high angular resolution *Chandra* observations by Pooley (2011) strongly suggest that the emission arose from a steady source 2.3 arcsec away from the SN. The most sensitive and constraining observation (prior to this event) was from a 20 ks *Chandra* observation of SN 2002bo, obtained 9 days past the explosion (Hughes et al. 2007). The 3σ upper limit was $L_X < 1.3 \times 10^{38} \text{ erg s}^{-1}$ (2–10 keV).

The *Swift* and *Chandra* X-ray observations of PTF 11kly provide the earliest (1 day) as well as the most sensitive limits (≈ 30 times deeper relative to previous upper limits) on X-ray emission from SNe Ia. As noted earlier (Section 3) there are two durable sources of X-ray emission: thermal bremsstrahlung and IC scattering of the SN photons by relativistic electrons. For such strong shocks, $kT = 10 \text{ keV}$ is a characteristic temperature (bremsstrahlung). IC scattering from 1 eV to the 0.1–10 keV band requires electrons with Lorentz factor γ in the range of 10–100, a reasonable range for strong (non-relativistic) shocks.

We first consider a model in which we ascribe all X-ray emission (if any) to thermal bremsstrahlung. Following the model discussed in Immler et al. (2006), $L_X = (\pi m^2)^{-1} \Lambda(T) (\dot{M}/w)^2 (vt)^{-1}$, and with the assumptions of an H+He plasma as in Section 2, $L_{\text{reverse}} = 30 L_{\text{forward}}$, and $\Lambda(T) = 3 \times 10^{-23} \text{ erg cm}^3 \text{ s}^{-1}$, the upper limit of $L_X < 4.4 \times 10^{36} \text{ erg s}^{-1}$ translates into a progenitor mass-loss constraint of $\dot{M} \lesssim 5 \times 10^{-6} w_7 M_\odot \text{yr}^{-1}$. Scaling from the upper limit for SN 2002bo, given the distinct and more conservative model assumptions of Hughes et al. (2007), suggests a limit for PTF 11kly of $\dot{M} \lesssim 4 \times 10^{-5} w_7 M_\odot \text{yr}^{-1}$.

Next, we consider the IC scattering model. From Chevalier & Fransson (2006) we find that the IC luminosity is

$$L_{\text{IC}} \approx 10^{36} \gamma_{\min} \left(\frac{\epsilon_e}{0.1}\right) v_9 t_d^{-1} \dot{M}_{-8} w_7^{-1} \left(\frac{L_{\text{SN}}}{10^{42} \text{ erg s}^{-1}}\right) \text{erg s}^{-1}, \quad (8)$$

²⁹ We use the convention of $X_n = X/10^n$ where it is assumed, unless explicitly specified, that the units are in CGS.

4. DISCUSSION

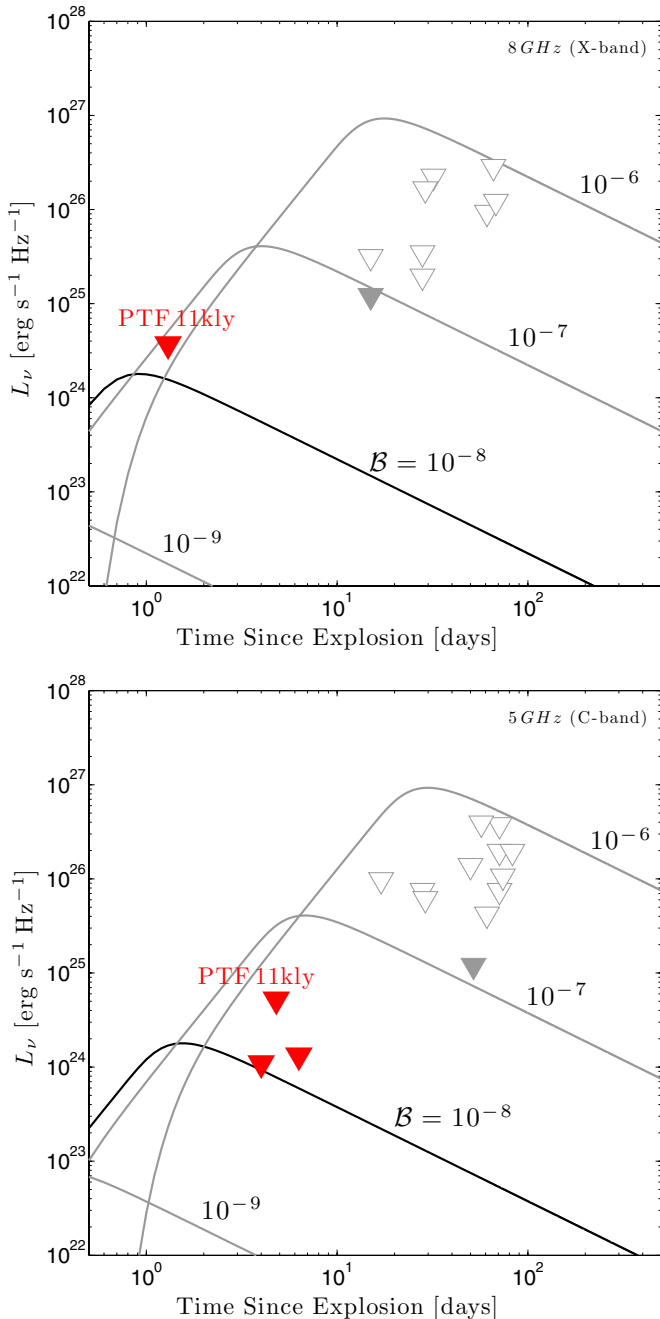


Figure 2. Model light curves for four different values of $B = \epsilon \dot{M}/w$ where $\epsilon^2 = \epsilon_B \epsilon_e$, w is the wind velocity, and \dot{M} is the mass-loss rate (see also Section 3.1). We assume the following normalization, $\epsilon = 0.1$, $w = 10^7 \text{ cm s}^{-1}$, and $v_s = 4 \times 10^9 \text{ cm s}^{-1}$. Model light curves for four values of $B = [10^{-6}, 10^{-7}, 10^{-8}, 10^{-9}] (0.1/\epsilon) w_7 M_\odot \text{ yr}^{-1}$ are shown. Top panel is for X band (8 GHz) while bottom panel is for C (5 GHz) band. The open triangles in both panels show upper limits from Panagia et al. (2006). The gray triangle in the top panel is the best limit from Panagia et al. (2006) while that in the bottom panel is the upper limit from Hancock et al. (2011). Red triangles are measurements of PTF11kly and presented in Table 1.

(A color version of this figure is available in the online journal.)

where L_{SN} is the bolometric luminosity from the SN. Clearly, the IC luminosity is independent of the highly variable ϵ_B and, unlike the radio luminosity (Equation (4)) has a gentle dependence on v_s . Assuming $\epsilon_e = 0.1$ and noting that $L_{\text{SN}} \sim 2 \times 10^{42} \text{ erg s}^{-1}$ on day 4 we find $\dot{M} \lesssim 10^{-8} w_7 M_\odot \text{ yr}^{-1}$ (90% confidence limit). Unlike the radio case this is a robust limit since it does not depend on ϵ_B .

As noted in Section 1 the commonly accepted SN Ia model is a thermonuclear explosion of a carbon+oxygen white dwarf close to the Chandrasekhar mass. However, such white dwarfs have masses smaller than the Chandrasekhar mass and so the Ia models necessarily involve the growth of mass of the WD. One such model is the coalescence of two WDs whose total mass is in the vicinity of the Chandrasekhar mass (see van Kerkwijk et al. 2010 and references therein). There is no expectation of an enriched CSM for (long-lived) DD systems. Thus the blast wave from the SN is not expected to produce any strong emission either in radio or X-ray bands.

On the other hand, in the SD model the WD can grow by a steady transfer of matter from a companion. This can occur from a close binary in Roche Lobe Overflow (RLOF), or by accretion directly from the wind of a companion (the symbiotic channel). In this class of models one may expect a CSM enriched by matter from the donor star either directly (by a wind from the donor star) or indirectly (matter that the WD is unable to accrete is expelled from the binary system).

It has long been the hope that early and sensitive radio and X-ray observations of nearby SNe Ia would diagnose the close-in circumstellar matter and thereby discriminate between the SD and DD models.

Here, we report the earliest radio and X-ray observations of PTF11kly and sensitive radio and X-ray observations undertaken by us and others at premier radio and X-ray facilities. Despite the sensitivity and rapidity no signal is seen at either radio or X-ray bands.

The absence of the signal is consistent with the expectation of the DD model but would hardly constitute proof of this channel. Below, we confront popular SD models with our null detection.

The radio observations find that $\dot{M} \lesssim 10^{-8} w_7 (0.1/\epsilon) M_\odot \text{ yr}^{-1}$, where $w = 10^7 w_7 \text{ cm s}^{-1}$ is the velocity with which the matter is ejected from the binary system and $\epsilon = \sqrt{\epsilon_B \epsilon_e}$. The X-ray observations yield an upper limit of $10^{-8} w_7^{-1} (0.1/\epsilon_e) M_\odot \text{ yr}^{-1}$. To our knowledge, these are the most sensitive limits on \dot{M} reported for any SN Ia to date.

Returning to the SD model, the growth in the mass of the WD is not assured. To start with, the mass transfer rate has to be high enough to prevent a nova explosion carrying off all the accreted matter. At high enough rates, steady burning can occur on the WD and the WD can grow in mass. Accretion at a rate of $\approx 10^{-7} M_\odot \text{ yr}^{-1}$ is thought to be necessary for stable accretion and nuclear burning on the surface of a WD (Nomoto 1982).

Systems in RLOF may achieve the required accretion rate—the class of binaries known as “supersoft X-ray sources” (van den Heuvel et al. 1992) show such behavior. But in addition to steady accretion, mass loss from the system is also thought to occur. Figure 1 from Han & Podsiadlowski (2004) gives theoretically expected mass-loss rates for the classical supersoft channel using the WD accretion efficiencies from Hachisu et al. (1999). In this phase, the mass loss from the system can reach $10^{-6} M_\odot \text{ yr}^{-1}$ and, in extreme (but rare) cases, more than $10^{-5} M_\odot \text{ yr}^{-1}$. The velocity of this material depends on the details of the ejection process; if it comes from the neighborhood of the WD, it is expected to be several 10^8 cm s^{-1} ; if it comes from a circum-binary envelope, its velocity should be at least of order the typical orbital velocity, i.e., a few 10^7 cm s^{-1} . Note, however, that in the vast majority of cases, the binary will not be in this wind phase at the time of explosion, and only a fraction of the mass transferred may be lost from the system at that time;

unfortunately, the exact amount is not well constrained by the theoretical models (perhaps a few $10^{-8} M_{\odot}$ with a velocity of at least a few 10^7 cm s^{-1}).

The radio limits for PTF 11kly do not rule out mass loss at that level. If the donor star is a main-sequence star or a slightly evolved sub-giant, its stellar wind is unlikely to be an important contribution to the systemic mass loss.

In the ‘‘symbiotic’’ SN Ia channel, the stellar wind from the donor star may be more important than mass loss associated with the mass-transfer process. If the companion is a Mira variable (in a D-type symbiotic), the expected mass loss is 10^{-6} to $10^{-4} M_{\odot} \text{ yr}^{-1}$ (e.g., Zijlstra 2006) with very low terminal velocity ($w \sim 10 \text{ km s}^{-1}$ or even less). Such high mass loss can clearly be ruled out in the case of PTF 11kly.

In an S-type symbiotic, which is a more likely SN Ia progenitor (Hachisu et al. 1999), the donor star is a much less evolved red giant with much lower mass loss. Seaquist & Taylor (1990) estimate typical rates of 10^{-8} to $10^{-7} M_{\odot} \text{ yr}^{-1}$ with large modeling uncertainties. A case of particular interest is the symbiotic binary EG And which contains an M2.4 red giant that is very similar to the red giant in the SN Ia candidate system RS Oph. The wind from EG And has a measured high terminal velocity of 75 km s^{-1} (Espey & Crowley 2008) with an uncertain estimate of the mass-loss rate of about $10^{-8} M_{\odot} \text{ yr}^{-1}$ (Crowley 2006). For comparison, the observed wind features in RS Oph have velocities in the range of $30\text{--}60 \text{ km s}^{-1}$ (Patat et al. 2011). In addition, observations of RS Oph show that the mass loss is very asymmetric and is strongly confined to the orbital plane (O’Brien et al. 2006), consistent with hydrodynamical modeling of the mass loss from such systems (Walder et al. 2008; S. Mohamed et al., in preparation). This introduces a possibly important viewing dependence of the radio signal. In this context, it is worth noting that these systems (both in the supersoft and the symbiotic channel) experience recurrent novae, typically every $10\text{--}20 \text{ yr}$ when the WD is close to the Chandrasekhar mass (Schaefer 2010), which may produce low-density cavities in the immediate CSM (Wood-Vasey & Sokoloski 2006). The upper limit for the mass-loss rate deduced from our radio limits for the progenitor of PTF 11kly is comparable to the expected mass loss from a symbiotic-like RS Oph. However, considering the uncertainties noted above, it may be premature to rule out such a system on the basis of these observations alone.

The limits we have derived from radio and X-ray observations on the progenitor system of PTF 11kly can be placed into context with complementary constraints from a variety of independent techniques. Li et al. (2011) examine pre-explosion *Hubble Space Telescope* images of M101 and derive limits on the brightness of any mass-donating companion. The lack of any optical emission at the location of PTF 11kly directly rules out luminous red giants and the vast majority of He stars, consistent with the limits we have derived here.

In summary, we present the most sensitive early radio and X-ray observations to date. Despite the rapid response and excellent sensitivity our observations can constrain only the symbiotic SD channel for PTF 11kly, but cannot rule out a main-sequence or sub-giant donor channel.

Prior observations which were both less sensitive and at later times nominally came to the same conclusion. However, the inference of \dot{M} from radio data depends on two microphysics parameters, ϵ_e and ϵ_B , and two velocities, v_s (shock speed) and w , the velocity with which matter is ejected from the binary system. In principle, v_s can be estimated from photospheric

velocities and a model for the exploding WD. The value of ϵ_e empirically shows modest variation and one can assume $\epsilon_e \approx 0.1$. However, ϵ_B , on empirical and theoretical grounds, can vary tremendously (with $\epsilon_B \approx 0.1$ being a maximum plausible value).

In the past, particularly in the radio literature, the assumed values were (in our opinion) rather optimistic: $w \sim 10^6 \text{ cm s}^{-1}$ and $\epsilon_B = 0.1$. Using the maximum possible value for $\epsilon_B \approx 0.1$, we find from our radio observations that $\dot{M} \lesssim 10^{-8} w_7 M_{\odot} \text{ yr}^{-1}$. Smaller values of ϵ_B will only make this limit worse (proportionally larger). Given that PTF 11kly was one of the closest SNe Ia it is not likely that the limits presented here would be bested in the near term.

The X-ray observations provide a less model dependent (and hence more robust) estimate of \dot{M} . The X-ray observations (especially if undertaken at peak) tightly constrain $\dot{M}\epsilon_e/w$. The microphysical parameter, ϵ_e , has far less dispersion as compared to ϵ_B and as such the X-ray observations yield a robust estimate of \dot{M} (relative to that obtained from radio observations). We find $\dot{M} \lesssim 10^{-8} w_7 M_{\odot} \text{ yr}^{-1}$. The X-ray observations are quite sensitive and it is not likely that these limits will be easily surpassed in this decade.

We thank the CARMA and EVLA staff for promptly scheduling this target of opportunity. This work made use of data supplied by the UK *Swift* Science Data Centre at the University of Leicester. We thank the ASTRON Radio Observatory for the generous and swift allocation of observing time. PTF is a fully automated, wide-field survey aimed at a systematic exploration of explosions and variable phenomena in optical wavelengths. The participating institutions are Caltech, Columbia University, Weizmann Institute of Science, Lawrence Berkeley Laboratory, University of Oxford, and University of California at Berkeley. The program is centered on a $12\text{K} \times 8\text{K}$, 7.8 square degree CCD array (CFH12K) re-engineered for the 1.2 m Oschin Telescope at the Palomar Observatory by Caltech Optical Observatories. Photometric follow-up is undertaken by the automated Palomar 1.5 m telescope. Research at Caltech is supported by grants from NSF and NASA. The Weizmann PTF partnership is supported in part by the Israeli Science Foundation via grants to A.G. Weizmann–Caltech Collaboration is supported by a grant from the BSF to A.G. and S.R.K. A.G. further acknowledges the Lord Sieff of Brimpton Foundation. M.M.K. acknowledges support from a Hubble Fellowship and Carnegie–Princeton Fellowship. We thank the ASTRON Radio Observatory for the generous and swift allocation of observing time. The Westerbork Synthesis Radio Telescope is operated by ASTRON (Netherlands Foundation for Radio Astronomy) with support from the Netherlands Organization for Scientific Research (NWO). A.J.v.d.H. was supported by NASA grant NNH07ZDA001-GLAST. S. B. C. acknowledges generous financial assistance from Gary & Cynthia Bengier, the Richard & Rhoda Goldman Fund, NASA/*Swift* grants NNX10AI21G and GO-7100028, the TABASGO Foundation, and NSF grant AST-0908886. A.K. is partially supported by NSF award AST-1008353.

REFERENCES

- Baars, J. W. M., Genzel, R., Pauliny-Toth, I. I. K., & Witzel, A. 1977, *A&A*, **61**, 99
 Björnsson, C.-I., & Fransson, C. 2004, *ApJ*, **605**, 823
 Boffi, F. R., & Branch, D. 1995, *PASP*, **107**, 347
 Chevalier, R. A. 1982, *ApJ*, **259**, 302
 Chevalier, R. A. 1998, *ApJ*, **499**, 810

- Chevalier, R. A., & Fransson, C. 2006, *ApJ*, **651**, 381
- Chomiuk, L., & Soderberg, A. 2011, *ATel*, **3532**, 1
- Crowley, C. 2006, PhD thesis, School of Physics, Trinity College Dublin, Dublin 2, Ireland
- Eck, C. R., Cowan, J. J., Roberts, D. A., Boffi, F. R., & Branch, D. 1995, *ApJ*, **451**, L53
- Espey, B. R., & Crowley, C. 2008, in ASP Conf. Ser. 401, RS Ophiuchi (2006) and the Recurrent Nova Phenomenon, ed. A. Evans, M. F. Bode, T. J. O'Brien, & M. J. Darnley (San Francisco, CA: ASP), 166
- Evans, P. A., Beardmore, A. P., Page, K. L., et al. 2009, *MNRAS*, **397**, 1177
- Feigelson, E. D., Broos, P., Gaffney, J. A., III, et al. 2002, *ApJ*, **574**, 258
- Fox, D. B. 2011a, *ATel*, **3592**, 1
- Fox, D. B. 2011b, *ATel*, **3593**, 1
- Fryer, C. L., Mazzali, P. A., Prochaska, J., et al. 2007, *PASP*, **119**, 1211
- Gal-Yam, A., Kasliwal, M. M., Arcavi, I., et al. 2011, *ApJ*, **736**, 159
- Hachisu, I., Kato, M., & Nomoto, K. 1999, *ApJ*, **522**, 487
- Han, Z., & Podsiadlowski, P. 2004, *MNRAS*, **350**, 1301
- Hancock, P. P., Gaensler, B. M., & Murphy, T. 2011, *ApJ*, **735**, L35
- Hillebrandt, W., & Niemeyer, J. C. 2000, *ARA&A*, **38**, 191
- Hoyle, F., & Fowler, W. A. 1960, *ApJ*, **132**, 565
- Hughes, J. P., Chugai, N., Chevalier, R., Lundqvist, P., & Schlegel, E. 2007, *ApJ*, **670**, 1260
- Hughes, J. P., Soderberg, A., & Slane, P. 2011, *ATel*, **3602**, 1
- Iben, I., Jr., & Tutukov, A. V. 1984, *ApJS*, **54**, 335
- Immler, S., Brown, P. J., Milne, P., et al. 2006, *ApJ*, **648**, L119
- Immler, S., & Russell, B. R. 2011, *ATel*, **3410**, 1
- Kalberla, P. M. W., Burton, W. B., Hartmann, D., et al. 2005, *A&A*, **440**, 775
- Kamphuis, J., Sancisi, R., & van der Hulst, T. 1991, *A&A*, **244**, L29
- Law, N. M., Kulkarni, S. R., Dekany, R. G., et al. 2009, *PASP*, **121**, 1395
- Li, W., Bloom, J. S., Podsiadlowski, P., et al. 2011, *Nature*, submitted (arXiv:1109.1593)
- Nomoto, K. 1982, *ApJ*, **253**, 798
- Nugent, P. E., et al. 2011, *Nature*, in press
- O'Brien, T. J., Bode, M. F., Porcas, R. W., et al. 2006, *Nature*, **442**, 279
- Pacholczyk, A. G. (ed.) 1970, *Radio Astrophysics: Nonthermal Processes in Galactic and Extragalactic Sources* (San Francisco, CA: W. H. Freeman)
- Panagia, N., Van Dyk, S. D., Weiler, K. W., et al. 2006, *ApJ*, **646**, 369
- Patat, F., Chugai, N. N., Podsiadlowski, P., et al. 2011, *A&A*, **530**, A63
- Perlmutter, S., Aldering, G., Goldhaber, G., et al. 1999, *ApJ*, **517**, 565
- Pooley, D. 2011, *ATel*, **3456**, 1
- Rau, A., Kulkarni, S. R., Law, N. M., et al. 2009, *PASP*, **121**, 1334
- Riess, A. G., Filippenko, A. V., Challis, P., et al. 1998, *AJ*, **116**, 1009
- Schaefer, B. E. 2010, *ApJS*, **187**, 275
- Seaquist, E. R., & Taylor, A. R. 1990, *ApJ*, **349**, 313
- Shappee, B. J., & Stanek, K. Z. 2011, *ApJ*, **733**, 124
- Soderberg, A. M., Brunthaler, A., Nakar, E., Chevalier, R. A., & Bietenholz, M. F. 2010, *ApJ*, **725**, 922
- Soderberg, A. M., Margutti, R., Zauderer, B. A., et al. 2011, arXiv:1107.1876
- van den Heuvel, E. P. J., Bhattacharya, D., Nomoto, K., & Rappaport, S. A. 1992, *A&A*, **262**, 97
- van Kerkwijk, M. H., Chang, P., & Justham, S. 2010, *ApJ*, **722**, L157
- Walder, R., Folini, D., & Shore, S. N. 2008, *A&A*, **484**, L9
- Webbink, R. F. 1984, *ApJ*, **277**, 355
- Weiler, K. W., Panagia, N., Montes, M. J., & Sramek, R. A. 2002, *ARA&A*, **40**, 387
- Whelan, J., & Iben, I., Jr. 1973, *ApJ*, **186**, 1007
- Wood-Vasey, W. M., & Sokoloski, J. L. 2006, *ApJ*, **645**, L53
- Yungelson, L. R., & Livio, M. 2000, *ApJ*, **528**, 108
- Zijlstra, A. A. 2006, in IAU Symp. 234, *Planetary Nebulae in Our Galaxy and Beyond*, ed. M. J. Barlow & R. H. Méndez (Cambridge: Cambridge Univ. Press), 55